JOURNAL OF MATERIALS SCIENCE 37 (2002) 249–256

# Proton conducting composites of heteropolyacid hydrates dispersed with salt hydrates

N. LAKSHMI, S. CHANDRA
*Department of Physics, Banaras Hindu University, Varanasi - 221 005, India*
*E-mail: schandra@banaras.ernet.in*

Proton conduction in the composites of heteropolyacid hydrates (Phosphotungstic acid : PTA·$n$$H_2O$ and Phosphomolybdic acid : PMA·$n$$H_2O$) with salt hydrates like Aluminium sulphate and Ammonium paratungstate (APT) as dispersoids has been studied and compared with the composites PTA : $Al_2O_3$ and PMA : $Al_2O_3$. Thermal analysis, XRD and IR studies on acid and salt hydrates dispersed phase systems reveal the formation of composites. A significant increase in the ionic conductivity has been observed in the composites. It has been found that the conductivity of $0.5PTA + 0.5Al_2(SO_4)_3 \cdot 16H_2O$ is $\sim 1.1 \times 10^{-2}$ S·cm$^{-1}$ and that of $0.55PMA + 0.45APT$ is $\sim 1.3 \times 10^{-3}$ S·cm$^{-1}$ at 65% R.H. The temperature and humidity dependence of bulk electrical conductivity of the composites is also reported. © *2002 Kluwer Academic Publishers*

## 1. Introduction

Proton conducting solids (belonging to the general class of solid electrolytes or superionic conductors or fast ion conductors) have gained importance due to their potential applications in electrochemical devices like fuel cells, batteries, sensors, electrochemical devices etc. [1–5]. Various methods have been employed to increase the conductivity of ionic conductors. Heterogeneous doping or formation of composites has been found to be an efficient method to improve the conductivity of ionic conductors with good mechanical properties. Since the discovery of substantial enhancement in the ionic conductivity in LiI:$Al_2O_3$ system by Liang [6], a large number of composite systems with $Li^+$, $Ag^+$, $Na^+$ ion conductors [7–10] have been reported but proton conducting composites are less studied. In general, the use of different insulating oxides like $Al_2O_3$, $SiO_2$, $ZrO_2$, $TiO_2$, fly ash etc. as dispersoids has been very successful for conductivity enhancement (2–4 orders) for $Li^+$, $Ag^+$, $Na^+$ conductors. However, only a limited success could be obtained in developing proton conducting composites using "oxides" as dispersoids. Recently, we studied PTA:$Al_2O_3$ and PMA:$Al_2O_3$ composites [11]. The conductivity enhancement is less than an order of magnitude. In proton conducting hydrates, the possible mobile species $H^+$ ($H_3O^+$) and $OH^-$ are highly reactive and it may lead to the formation of a new interfacial phase depending upon the nature of the insulating oxides (i.e. acidic, basic or amphoteric). The formation of the interface phase/compound may have a detrimental effect in the conductivity enhancement of the composites. Hence, the aim of the present study is to use other protonic conductors (but poor $\sigma$) as dispersoids in heteropolyacid hydrates Phosphotungstic acid [$H_3PW_{12}O_{40} \cdot nH_2O$:PTA] and Phosphomolybdic acid [$H_3PMo_{12}O_{40} \cdot nH_2O$:PMA]. The dispersoids chosen for the present study are Aluminium sulphate [$Al_2(SO_4)_3 \cdot 16H_2O$] and Ammonium paratungstate [$(NH_4)_{10}W_{12}O_{41} \cdot 2H_2O$:APT]. PMA:$Al_2(SO_4)_3 \cdot 16H_2O$ composite pellets are sticky and PTA:APT composites did not show any significant conductivity enhancement. Therefore, we undertook a systematic structural and electrical characterisation studies of PTA:$Al_2(SO_4)_3 \cdot 16H_2O$ and PMA:APT composites only which are given below.

## 2. Experimental

The materials employed were of analytical grade purity. Composites of different stoichiometric ratios were prepared by simple physical grinding method and pellets of 8 mm diameter were made at a pressure of 100 MPa for experimental studies. For structural characterisation, Differential Scanning Calorimetry (DSC)/Differential Thermal Analysis (DTA)/Thermogravimetric Analysis (TGA), X-ray Diffraction (XRD) and Infrared spectra have been taken for the pure materials and the composites.

DSC studies of PTA:$Al_2(SO_4)_3 \cdot 16H_2O$ were carried out using the DSC unit (Dupont 2100). The heating rate was kept at 5°C/min. DTA/TGA studies of PMA:APT have been carried out using Linseis DTA/TGA unit (Type 2045) at a heating rate of 5°C/min. Alumina powder was used as reference material. XRD patterns were recorded using X-ray diffractometer (Philips 1710). For IR spectra, the powdered sample was dispersed in KBr in the ratio 1:100 and pellets of 13 mm. diameter were made at about 800 MPa. The spectra were recorded using Perkin Elmer (model 883) IR spectrophotometer.

The total ionic transference number $t_{ion}$ was evaluated by Wagner's polarisation method [12]. A fixed small d.c. voltage (0.2 V) was applied across the sample

and the variation of current as a function of time was monitored. The electrical conductivity at different compositions, temperature and humidity was evaluated from the complex impedance plots using Solartron Frequency Response Analyser (1250) and an electrochemical interface (1286) coupled with a HP computer. The frequency range of measurement was 65 Hz–65 kHz. Graphite paste was used as the electrodes. Different supersaturated salt solutions were placed in a closed chamber to obtain different constant humidity levels.

## 3. Results and discussion

### 3.1. Thermal analysis

The DSC thermograms of pure PTA, pure $Al_2(SO_4)_3 \cdot 16H_2O$ and different composites $xH_3PW_{12}O_{40} \cdot nH_2O + (1-x)Al_2(SO_4)_3 \cdot 16H_2O$ with $x = 0.8$, 0.5 and 0.2 are shown in Fig. 1. The DSC record of pure PTA shows endothermic peaks at 75, 107 and 262°C. These peaks correspond to the removal of water molecules from the lattice. In pure $Al_2(SO_4)_3 \cdot 16H_2O$, a sharp endothermic peak appears at 121°C which has been attributed to the self dissolution of aluminium sulphate in its own outgoing water of crystallisation [13]. The small endothermic peak at 162°C is linked to loss of water of crystallisation. The DSC thermograms of the composites do not show the presence of any new peak and the peaks correspond to either pure PTA or $Al_2(SO_4)_3 \cdot 16H_2O$. It is found that the peaks due to PTA or $Al_2(SO_4)_3 \cdot 16H_2O$ get weakened as their relative respective amounts change in the different composites. In the composite with $x = 0.8$, endothermic peaks appear at 70, 110, 124, 152 and 248°C. All these peaks correspond to either PTA or $Al_2(SO_4)_3 \cdot 16H_2O$. At $x = 0.5$, endothermic peaks appear at 70 and 172°C. Similarly, at $x = 0.2$, a sharp endothermic peak is seen at 126°C corresponding to $Al_2(SO_4)_3 \cdot 16H_2O$ whose amount is higher in the composite. Weak shoulders appear at 77 and 100°C (very weak and only seen as an asymmetry in the major peak at 120°C) and a broad hump at ~175–195°C also occurs. Thus, the DSC data indicates the formation of composites without any new interface compound formation.

The DTA/TGA records of pure PMA, APT and a representative composition $x\text{PMA} + (1-x)\text{APT}$ ($x = 0.55$) of the composite are shown in Fig. 2 The

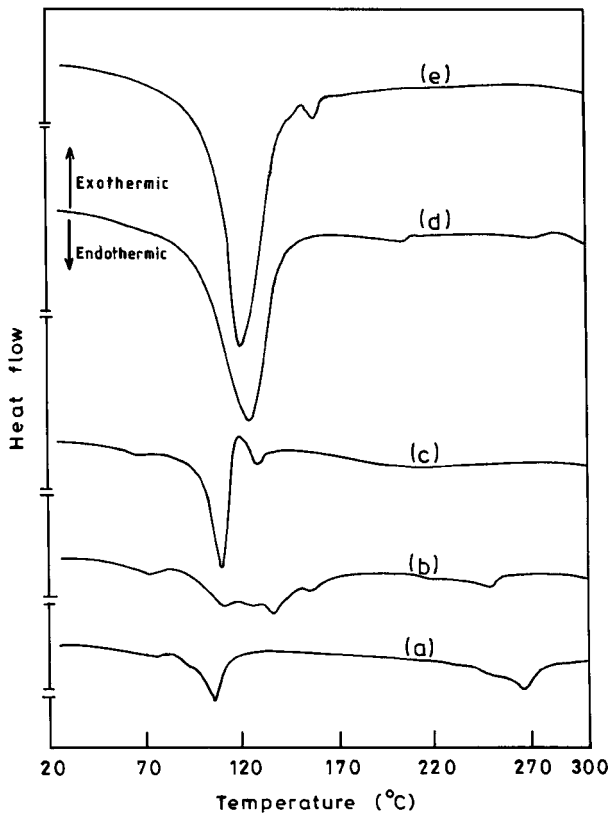


*Figure 1* DSC records of (a) pure PTA, (b–d) $x\text{PTA} + (1-x)Al_2(SO_4)_3 \cdot 16H_2O$ composites with $x = 0.8$, 0.5 and 0.2 respectively and (e) pure $Al_2(SO_4)_3 \cdot 16H_2O$.

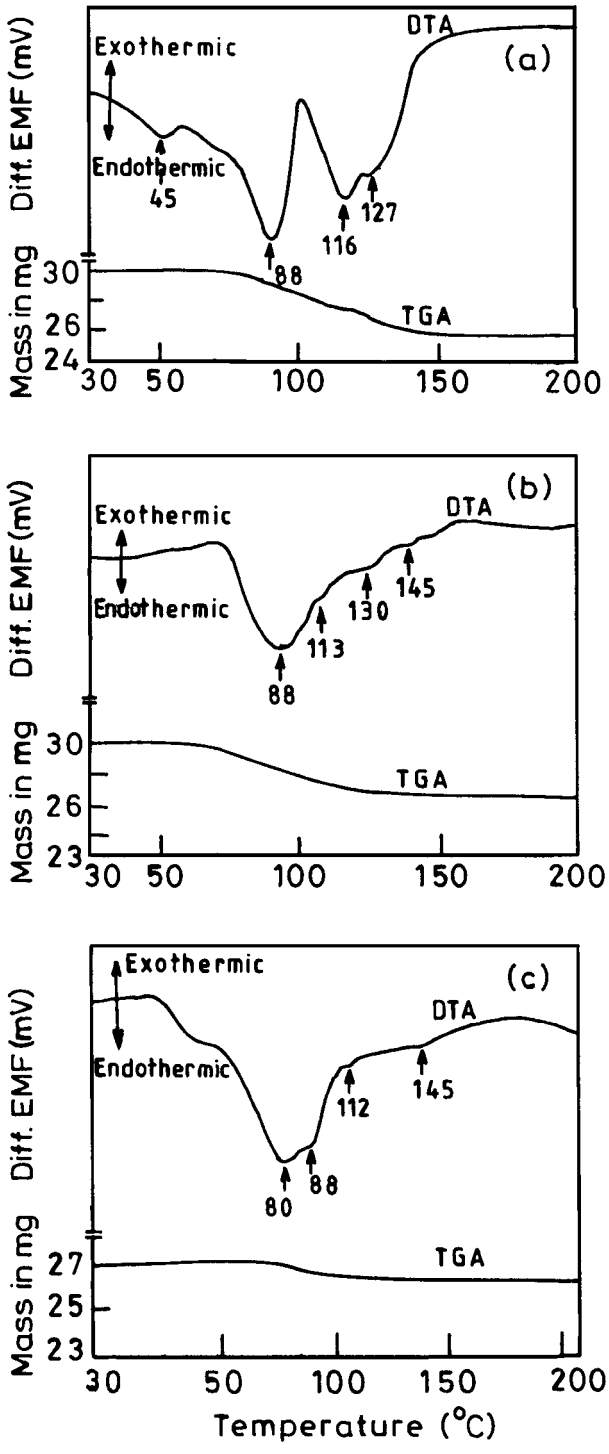


*Figure 2* DTA/TGA records of (a) pure PMA, (b) 0.55PMA + 0.45APT composite and (c) pure APT.

DTA record of pure PMA shows endothermic peaks at 45, 88, 116 and 127°C. The peak at 45°C is attributed to the removal of surface adsorbed water molecules and the rest of the peaks correspond to the removal of water molecules from the lattice. The TGA trace also shows weight loss. The values of $\Delta m/m$ ($\Delta m$ is the change in mass of the proton conducting sample due to dehydration and $m$ is the mass of PMA in the sample) obtained from the TGA curve is found to be 0.15. The DTA record of APT shows endothermic peaks at 45, 80, 88, 112 and 145°C. The broad endothermic peak at 45°C corresponds to the removal of physisorbed water molecules whereas the rest of the peaks are attributed to the loss of water of crystallisation from the lattice. The $\Delta m/m$ value from the TGA record is found to be 0.05. In the $x$PMA + $(1-x)$APT composite with $x = 0.55$, the DTA record shows endothermic peaks at 88, 113, 130 and 145°C which corresponds to the removal of water molecules from the lattice. The $\Delta m/m$ value is found to be 0.06. The DTA record of the composite does not show the presence of any new peak and all the peaks in the composite correspond either to pure PMA or APT. Thus, the DTA/TGA confirms the formation of composites and does not indicate the formation of any new interface compound for the case of PMA:APT system also.

## 3.2. Infrared studies

The infrared spectra of different compositions of $x H_3PW_{12}O_{40}\cdot nH_2O + (1-x)Al_2(SO_4)_3\cdot 16H_2O$ are shown in Fig. 3. A broad band observed in the region 3600–3000 $cm^{-1}$ in pure PTA, $Al_2(SO_4)_3\cdot 16H_2O$ and PTA:$Al_2(SO_4)_3\cdot 16H_2O$ composites is assigned to the ─OH stretching mode [14]. The band at ~2539 $cm^{-1}$ in $Al_2(SO_4)_3\cdot 16H_2O$ and the composites is associated with H─O─H stretching [15]. A small peak appears at ~1704 $cm^{-1}$ in pure PTA which is assigned to the asymmetric stretching vibration of O─H─O in $H_5O_2^+$ [16, 17]. Mioc *et al.* [18] assigned the band at ~1720 $cm^{-1}$ to $\nu(H_3O^+)$ whereas Jones *et al.* [19] attributed it to the deformation of $H_2O$ group in $H_5O_2^+$. If $H_5O_2^+$ is asymmetric, then the description in terms of $H_3O^+$─$H_2O$ or $H_5O_2^+$ is identical [18]. In the composites with $x = 0.9$ and 0.8, the peak of ~1704 $cm^{-1}$ appears only as a shoulder and gradually disappears at higher $Al_2(SO_4)_3\cdot 16H_2O$ concentrations. The band at ~1620 $cm^{-1}$ in PTA, $Al_2(SO_4)_3\cdot 16H_2O$ and the composites can be assigned to HOH bending [14]. A weak band appears at ~1404 $cm^{-1}$ in pure PTA which can be assigned to the H─O─H asymmetric deformation [16, 20]. This peak also gradually disappears in the composites having less PTA.

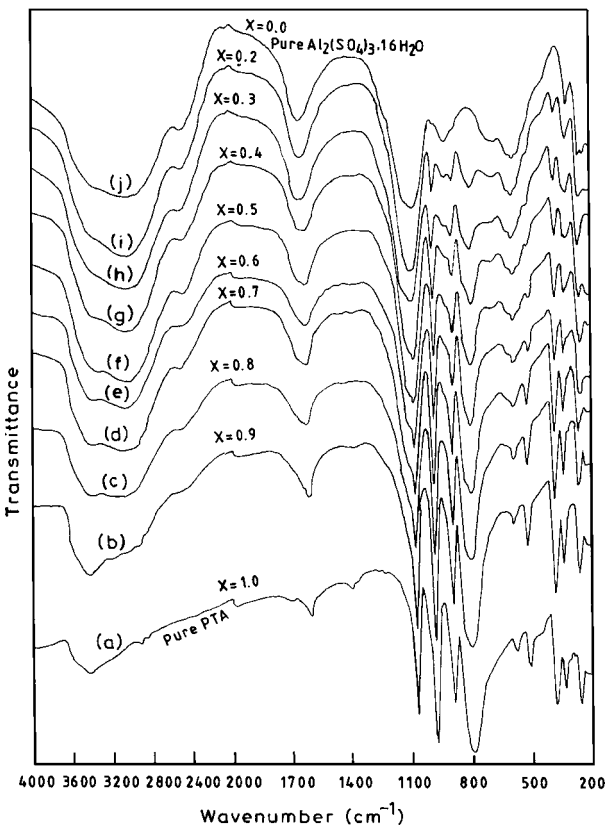


*Figure 3* IR spectra of (a) pure PTA, (b–i) $x$PTA + $(1-x)Al_2(SO_4)_3\cdot 16H_2O$ composites with $x = 0.9$, 0.8, 0.7, 0.6, 0.5, 0.4, 0.3 and 0.2 respectively and (j) pure $Al_2(SO_4)_3\cdot 16H_2O$.

Four well defined sharp peaks appear in pure PTA and its composites at ~1080, 985, 891 and 800 $cm^{-1}$ characteristic of the Keggin structure of $PW_{12}O_{40}^{3-}$ [21, 22]. The strong absorption band at ~1080 $cm^{-1}$ in pure PTA is assigned to the asymmetric stretching of the $\nu_3(PO_4)$ group. A broad band at ~1100 $cm^{-1}$ in aluminium sulphate can be assigned to the $\nu_3$ mode of $(SO_4)^{2-}$ [13]. In the composites, a strong absorption band appears at ~1090 $cm^{-1}$ associated with the $\nu_3$ mode of sulphate and phosphate groups of aluminium sulphate and PTA respectively. The sharp bands at ~985, 891 and 800 $cm^{-1}$ in PTA and the composites are assigned to the asymmetric stretching of W═O, W─$O_b$─W and W─$O_c$─W respectively [21, 23]. A weak band at ~990 $cm^{-1}$ in pure aluminium sulphate and the composites with higher concentrations of $Al_2(SO_4)_3\cdot 16H_2O$ is associated with $\nu_1(SO_4)^{2-}$ [14]. A small band at ~695 $cm^{-1}$ in $Al_2(SO_4)_3\cdot 16H_2O$ corresponds to Al─OH rocking [13]. This band gradually reduces to a shoulder in the composites with less $Al_2(SO_4)_3\cdot 16H_2O$.

The small peak at ~581 $cm^{-1}$ in pure PTA is attributed to the $\nu_4$ deformation mode of free $PO_4^{3-}$ ion [24]. A small shoulder at ~618 $cm^{-1}$ and a band at ~590 $cm^{-1}$ in aluminium sulphate is associated with $\nu_4(SO_4)^{2-}$ [14] and Al─OH wagging [13] respectively. Hence, in the composites the shoulder at ~618 $cm^{-1}$ corresponds to $\nu_4(SO_4)^{2-}$ and the band at ~580 $cm^{-1}$ can be due to the combined effect of $\nu_4$ of $PO_4^{3-}$ and Al─OH wagging. The small band at ~515 $cm^{-1}$ in pure PTA attributed to asymmetric bending of $PO_4$ group [23] is gradually reduced to a weak intensity peak in the composites. A band at ~375 $cm^{-1}$ in pure PTA and the composites is attributed to the combined symmetric and asymmetric bending of $PO_4$ [23]. The peak at ~332 $cm^{-1}$ and the peak at ~320 $cm^{-1}$ in $Al_2(SO_4)_3\cdot 16H_2O$ can be assigned to the mixed deformation of O─W─O [23] and Al─OH twisting [13] respectively. Hence, the peak at ~325 $cm^{-1}$ in the composites may be due to both. The small band at ~257 $cm^{-1}$ in PTA and the composites can be assigned to O─W─O mixed deformations.

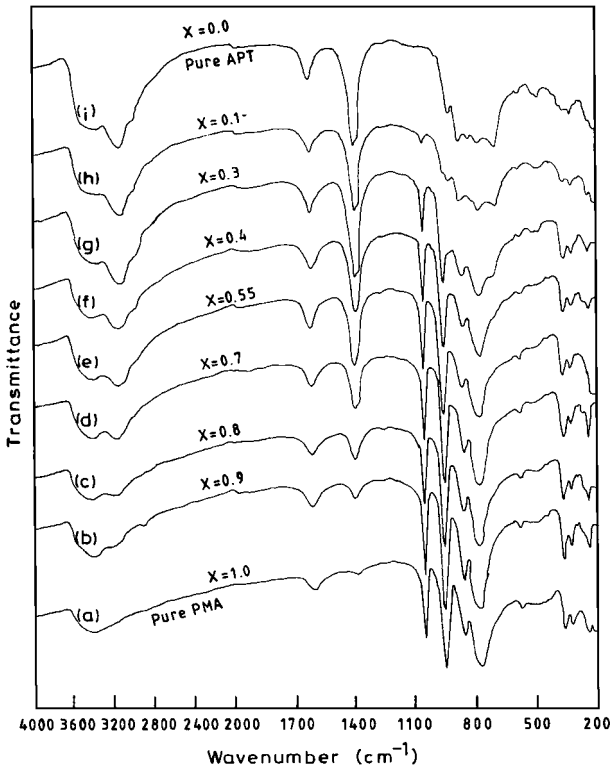


*Figure 4* IR spectra of (a) pure PMA, (b–h) $x$PMA + $(1-x)$APT composites with $x = 0.9$, 0.8, 0.7, 0.55, 0.4, 0.3 and 0.1 respectively and (i) pure APT.

Results on PMA:APT composites are qualitatively similar to those of PTA:$Al_2(SO_4)_3{\cdot}16H_2O$ composites discussed above. The infrared spectra of different compositions of $xH_3PMo_{12}O_{40}{\cdot}nH_2O + (1-x)(NH_4)_{10}W_{12}O_{41}{\cdot}2H_2O$ are shown in Fig. 4. A broad band observed around ~3600–3100 cm$^{-1}$ in PMA is assigned to the ─OH stretching mode [14]. The band at ~3440 cm$^{-1}$ in APT and the composites can be assigned to ─OH stretching and $NH_4^+$, N─H stretching [14]. The band at ~1625 cm$^{-1}$ is associated with HOH bending [14]. A small peak at ~1410 cm$^{-1}$ in pure PMA is assigned to H─O─H asymmetric deformation mode [16, 20]. The band at ~1403 cm$^{-1}$ in APT and the composites corresponds to $\nu_4(NH_4^+)$ [14]. The bands at ~1065, 964, 870 and 785 cm$^{-1}$ in PMA are characteristic of the keggin unit $(PMo_{12}O_{40})^{3-}$ [25]. The strong absorption band at ~1065 cm$^{-1}$ and the band at ~962 cm$^{-1}$ in PMA and the composites is assigned to the $\nu_3$ mode of $PO_4$ and Mo═O vibration. A weak band appears at ~936 cm$^{-1}$ in APT and also in the composite with $x = 0.1$ associated with $\nu_1(WO_4)^{2-}$ [14]. The band at ~870 cm$^{-1}$ in pure PMA corresponds to Mo─O─Mo vibration whereas the band at ~884 cm$^{-1}$ in APT can be assigned to W─OH [26]. Hence, the band around 874 cm$^{-1}$ in the composites may be due to both the above. The band at ~785 cm$^{-1}$ in PMA can be assigned to Mo─O─Mo and the band at ~789 cm$^{-1}$ in APT may be assigned to W─O─W. In the composites, a single peak appears at ~788 cm$^{-1}$ corresponding to the above. A small band at ~585 cm$^{-1}$ in pure PMA and its composites is associated with $\nu_4$ deformation of $PO_4^{3-}$ ion [24].

The absorption band at ~374 cm$^{-1}$ in pure PMA and its composites is assigned to the combined symmetric and asymmetric bending of $PO_4$ group [23]. The bands at ~335 and 250 cm$^{-1}$ can be assigned to the metal - oxygen vibrations [23, 25, 27].

Thus, the IR studies indicate that no new peaks other than those of PMA/PTA and $Al_2(SO_4)_3{\cdot}16H_2O$/APT appear after the formation of composites.

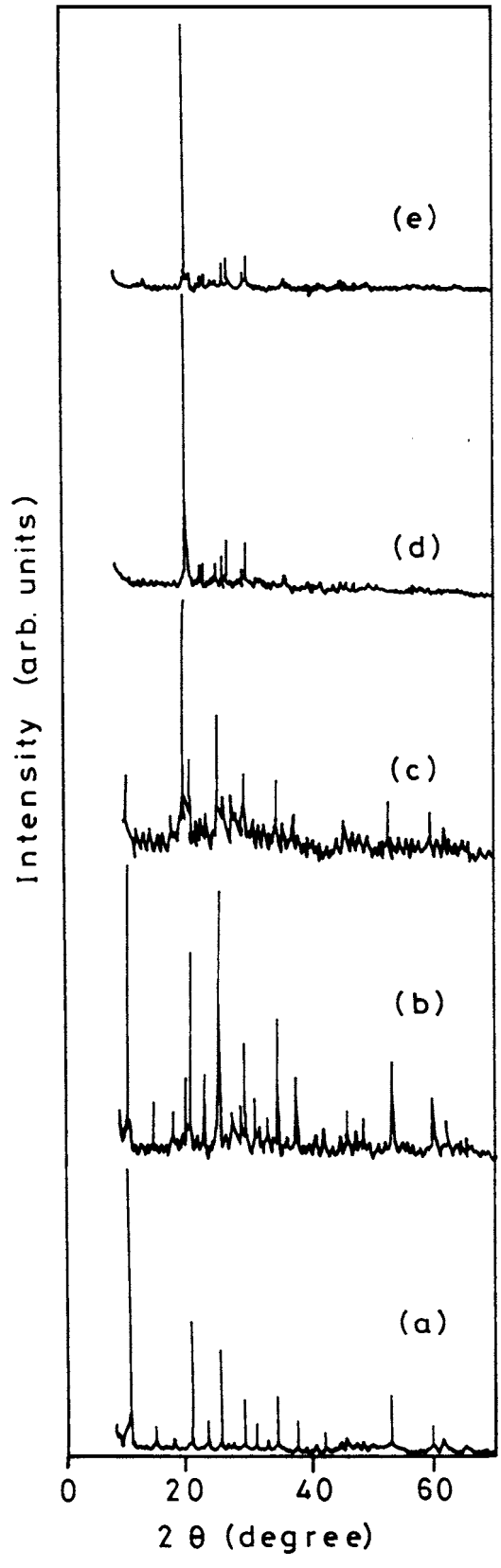


*Figure 5* XRD patterns of (a) pure PTA, (b–d) $x$PTA + $(1-x)$ $Al_2(SO_4)_3{\cdot}16H_2O$ composites with $x = 0.8$, 0.5 and 0.2 respectively and (e) pure $Al_2(SO_4)_3{\cdot}16H_2O$.

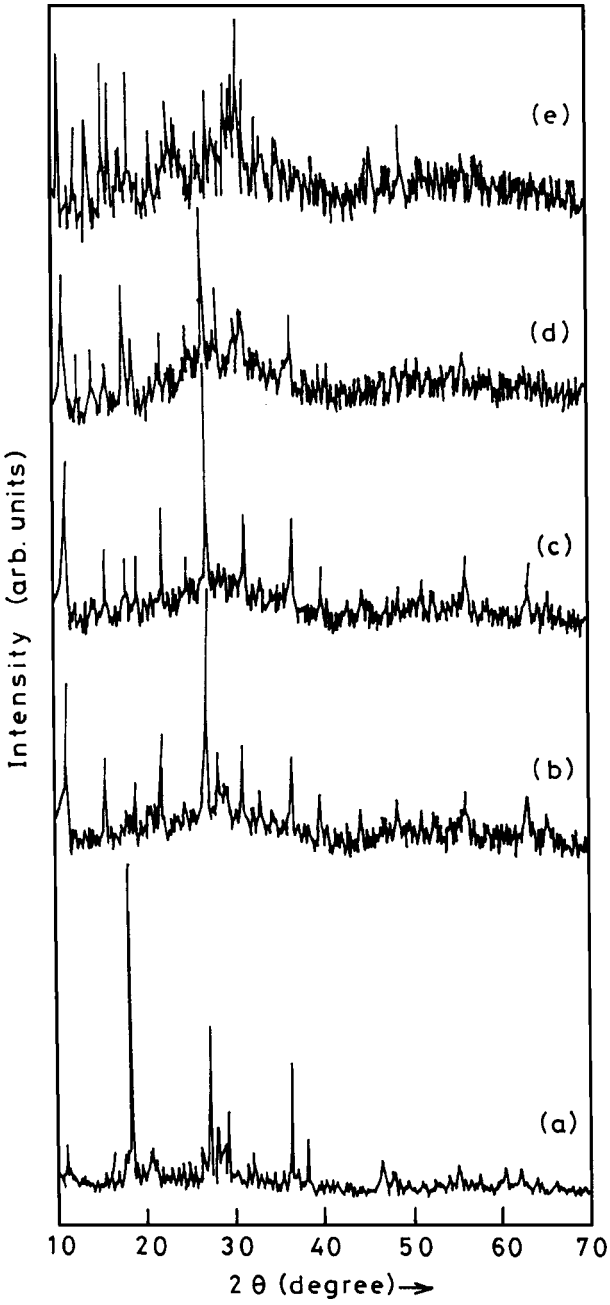


*Figure 6* XRD patterns of (a) pure PMA, (b–d) $x$PMA + $(1-x)$APT composites with $x = 0.8$, 0.55 and 0.3 respectively and (e) pure APT.

### 3.3. XRD studies

The X-ray diffraction patterns of different compositions of $x$PTA + $(1-x)$ $Al_2(SO_4)_3{\cdot}16H_2O$ and $x$PMA + $(1-x)$APT are shown in Figs 5 and 6. The diffraction patterns show well defined peaks indicating the crystalline nature of the material. The peaks appearing in the composites correspond to either of the pure host materials and no new peak is observed. Thus, the XRD studies support the conclusions of the thermal analysis and IR that no new interface compound is formed as observed in the case of PMA/PTA:$Al_2O_3$ composites [11] and the two phases exist separately.

### 3.4. Total ionic transference number

The total ionic transference number of typical compositions of the composites 0.5PTA + 0.5$Al_2(SO_4)_3{\cdot}$ $16H_2O$ and 0.55PMA + 0.45APT was evaluated using

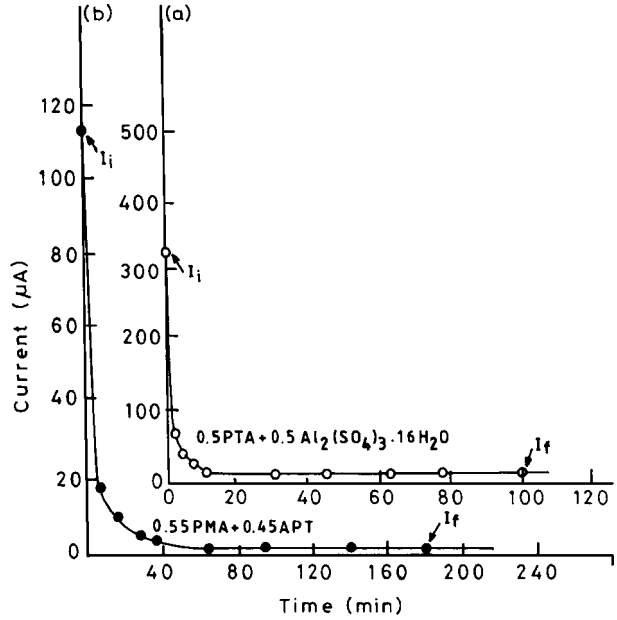


*Figure 7* The current vs. time plots in a typical Wagner's polarisation experiment for (a) 0.5PTA + 0.5$Al_2(SO_4)_3{\cdot}16H_2O$ and (b) 0.55PMA + 0.45APT composites.

Wagner's polarisation method. The current vs. time plots are shown in Fig. 7. It is found that the composites are predominantly ionic with $t_{ion} \sim 0.99$.

### 3.5. Composition dependence of conductivity

Fig. 8a and b shows the variation of bulk electrical conductivity with composition of PTA:$Al_2(SO_4)_3{\cdot}$ $16H_2O$ and PMA : APT systems. In the case of PTA: $Al_2(SO_4)_3{\cdot}16H_2O$, the conductivity increases with the addition of the dispersoid $Al_2(SO_4)_3{\cdot}16H_2O$ and the maximum conductivity ($1.1 \times 10^{-2}$ S·cm$^{-1}$; R.H. = 65%) is for the optimum composition with $x = 0.5$ and then decreases with further addition of $Al_2(SO_4)_3{\cdot}16H_2O$. There is also a small maxima at $\sim x = 0.7$. Similarly, for $x$PMA + $(1-x)$APT composite, the maximum conductivity ($3.9 \times 10^{-4}$ S·cm$^{-1}$; R.H. = 55%) is for $x = 0.55$. The second maxima (around $x = 0.8$) is not so clear. For the purpose of comparison of acid hydrates : salt hydrates composites with those of acid hydrates : insulating $Al_2O_3$ composites, the $\sigma$ vs. composition for the latter is given in Fig. 8c and d. The following points emerge:

(i) The overall conductivity enhancements in insulating $Al_2O_3$ dispersed in PMA or PTA is less as compared to those being respectively dispersed with another proton conducting hydrate APT or $Al_2(SO_4)_3{\cdot}16H_2O$. The best composite is PTA:$Al_2(SO_4)_3{\cdot}16H_2O$ with a room temperature conductivity as high as $\sim 10^{-2}$ S·cm$^{-1}$ and amounts to $\sim$2 orders of magnitude enhancement in $\sigma$. The reason for $Al_2O_3$ being less effective as dispersoid for conductivity enhancement in proton conducting composites can be explained on the basis of reaction of mobile $H^+$ or $OH^-$ protonic species with the amphoteric $Al_2O_3$ leading to an interface compound formation. In fact, such interface compound formation has been earlier detected by us from XRD studies [11]. There is no loss of mobile charge protonic

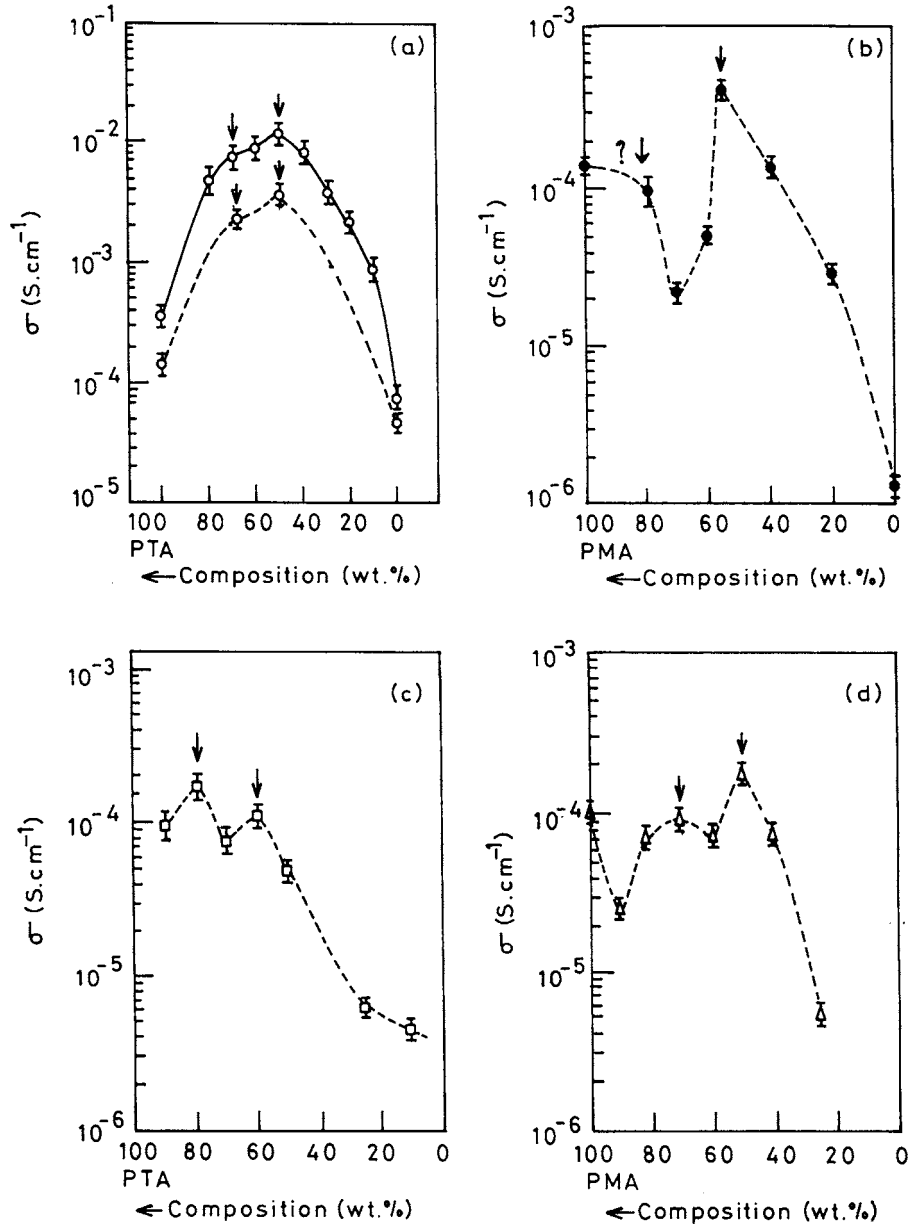


*Figure 8* Composition dependence of room temperature bulk conductivity of (a) PTA:$Al_2(SO_4)_3{\cdot}16H_2O$, (b) PMA:APT, (c) PTA:$Al_2O_3$ and (d) PMA:$Al_2O_3$ composite systems. The solid (—) line is for R.H. ~65% and the dotted (---) line is for R.H. ~55%.

species for the present cases of PTA:$Al_2(SO_4)_3{\cdot}16H_2O$ or PMA:APT composites as a result of absence of any such interface reaction.

(ii) Evidence exists for two peaks in $\sigma$ vs. composition plots in all the proton conducting composites. The conductivity enhancement, in general, is understood in terms of well known adsorption - desorption model of Maier [8] coupled with the percolation threshold concept given by Bunde *et al.* [28, 29] for ion conducting composites. The ion conducting matrix (PMA/PTA) possibly consists of two kinds of mobile species ($H^+/H_3O^+$ or $OH^-$) and the two species follow different thresholds and the sum of the two results in two maxima. Zhu and Mellander [30] also found two maxima in $RbNO_3$:$Al_2O_3$ at high temperatures and explained on the basis of mobility of $Rb^+$ and interfacial proton ($H^+$) conduction. The other possible "alternative" explanation in terms of the formation of some new high conducting interface compound getting formed at the PMA/PTA:$Al_2O_3$ interface may be considered as plausible (but not necessarily true) for PMA/PTA:$Al_2O_3$ composites in view of our earlier studies [11] but this explanation is not even tenable for the present case since there does not exist any evidence for the formation of any interface compound.

## 3.6. Temperature dependence of conductivity

The variation of electrical conductivity as a function of temperature for 0.5PTA + 0.5$Al_2(SO_4)_3{\cdot}16H_2O$ and 0.55PMA + 0.45APT composites are shown in Fig. 9. In the $\sigma$ vs. $1/T$ plot of PTA:$Al_2(SO_4)_3{\cdot}16H_2O$ composite, the conductivity initially increases up to 50°C. The $\sigma$ vs. $1/T$ plot in this temperature range 25–50°C is linear and suggests an Arrhenius type thermally activated process with $E_a = 0.21$ eV. Above 50°C, the rate of increase of $\sigma$ decreases and beyond 90°C, the conductivity falls rapidly as a result of dehydration of the material due to the removal of water molecules from

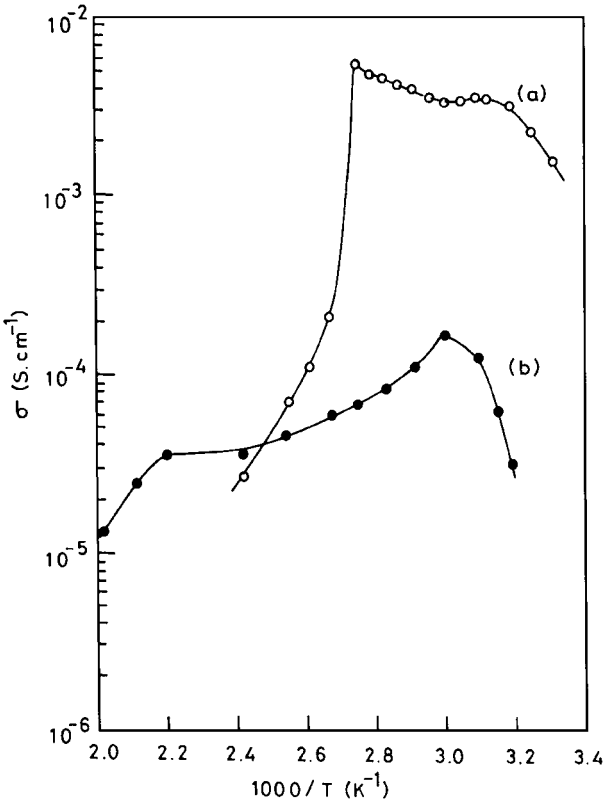


*Figure 9* Variation of $\sigma$ with temperature for (a) 0.5PTA + 0.5$Al_2(SO_4)_3 \cdot 16H_2O$ and (b) 0.55PMA + 0.45APT composites.

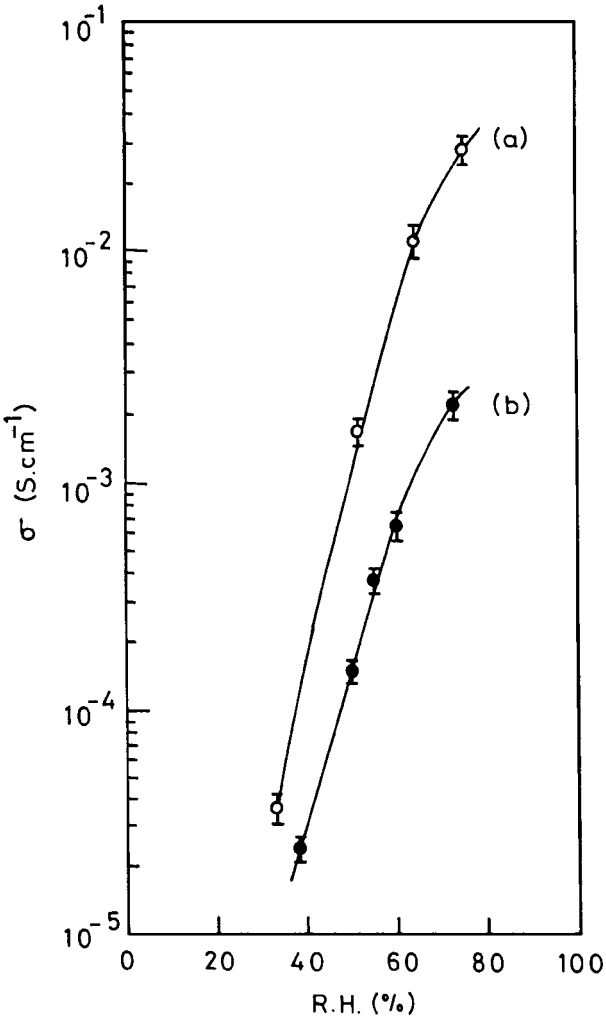


*Figure 10* Variation of $\sigma$ with relative humidity of (a) 0.5PTA + 0.5$Al_2(SO_4)_3 \cdot 16H_2O$ and (b) 0.55PMA + 0.45APT composites.

the lattice. In 0.55PMA + 0.45APT composite, the conductivity increases up to 60°C. The $\sigma$ vs. $1/T$ plot in 30–60°C temperature range is linear suggesting an Arrhenius behavior with $E_a = 0.52$ eV. Above 60°C, the conductivity decreases gradually until 180°C associated with loss of water molecules and above 180°C, $\sigma$ falls rapidly. The decrease in conductivity at high temperatures in all these cases is due to the dehydration of hydrates used which, in turn, reduces the number of available mobile protonic species.

### 3.7. Humidity dependence of conductivity

Fig. 10 shows the variation of electrical conductivity as a function of relative humidity of 0.5PTA + 0.5$Al_2(SO_4)_3 \cdot 16H_2O$ and 0.55PMA + 0.45APT. It has been found that the conductivity depends on humidity which is typical of proton conducting materials.

## 4. Conclusions

Proton conducting composites PTA:$Al_2(SO_4)_3 \cdot 16H_2O$ and PMA:APT are predominantly ionic. The DSC/DTA/TGA, IR and XRD studies confirm the formation of composites and do not indicate the formation of any new interface compound. Dispersion of other proton conducting hydrates in contrast to insulating oxides appears a better alternative since it results in more enhancement in the conductivity of the composites. The $\sigma$ vs. $1/T$ plots show an Arrhenius behaviour in a limited temperature range and closely follows the dehydration pattern as deduced from the thermal analysis. The values of $\sigma$ also depend upon humidity as expected for proton conducting hydrates.


## Acknowledgements

Thanks are due to CSIR, New Delhi for providing Senior Research Fellowship to NL and Emeritus Scientist project to SC.


## References


1. S. CHANDRA, *Material Science Forum* **1** (1984) 153; S. CHANDRA, in "Superionic Solids and Solid Electrolytes—Recent Trends," edited by A. L. Laskar and S. Chandra (Academic Press, New York, 1989) p. 185.
2. *Idem.*, in "Handbook of Solid State Batteries and Capacitor," edited by M. Z. A. Munshi (World Scientific, Singapore, 1995) p. 579.
3. Pselectfonth. COLOMBAN (ed.), "Proton Conductors: Solids, Membranes and Gels—Materials and Devices" (Cambridge Univ. Press, Cambridge, UK, 1992).
4. K. D. KREUER, *Chem. Mat.* **8** (1996) 610.
5. Pselectfonth. COLOMBAN, *Ann. Chem. Soc. Mat.* **24** (1999) 1.
6. C. C. LIANG, *J. Electrochem. Soc.* **120** (1973) 1289.
7. K. SHAHI and J. B. WAGNER Jr., *Solid State Ionics* **3/4** (1981) 295.
8. J. MAIER, *J. Phys. Chem. Solids* **46** (1985) 309.
9. *Idem.*, *Prog. Solid State Chem.* **23** (1995) 171.
10. A. LUNDEN, B.-E. MELLANDER, A. BENGTZELIUS, H. LJUNGMARK and R. TARNRBERG, *Solid State Ionics* **18/19** (1986) 514.
11. N. LAKSHMI and S. CHANDRA, *Phys. Stat. Solidi* (a) **186** (2001) 383.
12. J. B. WAGNER Jr. and C. WAGNER, *J. Chem. Phys.* **26** (1957) 1579.
13. T. SATO, F. OZAWA and S. IKONA, *J. Appl. Chem. Biotechnol.* **28** (1978) 811.

14. K. NAKAMOTO (ed.), "Infrared and Raman Spectra of Inorganic and Coordination Compounds" (John Wiley and Sons, New York, 1986).
15. G. M. MURPHY, G. WEINER and J. J. OBERLY, *J. Chem. Phys.* **22** (1954) 1322.
16. G. J. KEARLEY, H. A. PRESSMAN and R. C. T. SLADE, *J. Chem. Soc. Chem. Commun.* (1986) 1801.
17. A. C. PAVIA and P. A. GIGUERE, *J. Chem. Phys.* **52** (1970) 3551.
18. U. MIOC, M. DAVIDOVIC, N. TJAPKIN, Ph. Colomban and A. Novak, *Solid State Ionics* **46** (1991) 103.
19. D. J. JONES, J. ROZIERE, J. PENFOLD and J. TOMKINSON, *J. Mol. Struct.* **195** (1989) 283.
20. G. J. KEARLEY, R. P. WHITE, C. FORANO and R. C. T. SLADE, *Spectrochim Acta* **A46** (1990) 419.
21. C. ROCCHICCIOLI-DELTCHEFF, M. FOURNIER and R. FRANCK, *Inorg. Chem.* **22** (1983) 207.
22. D. H. BROWN, *Spectrochim Acta* **19** (1963) 585.
23. S. S. SALEEM and G. ARULDHAS, *Ind. J. Pure and Appl. Phys.* **21** (1983) 112.
24. A. C. CHAPMAN, D. A. LONG and D. T. L. DONES, *Spectrochim Acta*, **24** (1965) 633.
25. C. ROCCHICCIOLI-DELTCHEFF, R. THOUVENOT and R. FRANCK, *ibid.* **A32** (1976) 587.
26. A. B. KISS, P. GADO and A. J. HEGEDUS, *Acta Chimica Academiae Scientiarum Hungaricae* **72** (1972) 371.
27. W. P. GRIFFITH and T. D. WICKINS, *J. Chem. Soc.* A (1968) 400.
28. A. BUNDE, W. DIETERICH and E. ROMAN, *Solid State Ionics* **18/19** (1986) 147.
29. A. BUNDE, *ibid.* **75** (1995) 147.
30. B. ZHU and B-E. MELLANDER, *ibid.* **77** (1995) 244.

*Received 11 April*
*and accepted 3 August 2001*